Comparison of mapped and synthetic inflow boundary conditions in Direct Numerical Simulation of sprays

R. Payri, [1], F. J. Salvador, J. Gimeno, M. Crialesi-Esposito*
[1]CMT-Motores Térmicos, Universitat Politècnica de València, Spain.
*Corresponding author: marcres@mot.upv.es

1 Abstract

Direct Numerical Simulation (DNS) is getting more and more relevant in numerical analysis of sprays allowing insight on breakup mechanism, granulometry studies and analysis of the turbulence field. While for more fundamental studies the flow inlet boundary conditions are often neglected, it is mandatory for real application analysis to use reliable boundary condition in order to replicate as faithfully as possible the physical phenomena. On the other hand, the exact solution for many nozzles of engineering interest is unknown, hence there is a tendency to use simplified boundary conditions, such as the ones generating synthetic turbulence, as a simpler way to approach sprays DNS simulations without falling into the uncertainties of the nozzle flows.

In this framework, this work presents a comparison between DNS simulations in Paris-Simulator using both a digital filter based synthetic turbulence inflow boundary conditions against the mapped results generated by a Large Eddy Simulation of a periodic pipe flow. Both simulations will be carried at a Re=5050 and with physical parameters resembling the Spray A configuration given by the Engine Combustion Network. The main aim of the work is to understand how the longitudinal turbulence structures developed inside the nozzle are affecting the atomization regime and the breakup mechanism. This analysis is supported by an in-depth comparison of the resulting granulometry for both simulations.

After providing an in-depth analysis of the flow behaviour, the conclusions will be aiming to drawn some useful considerations on what are the main implications of the two approaches and whether or not synthetic boundary conditions are feasible for engineering studies, where usually the degree of complexity of the flow features outside the nozzle is more stringent than theoretical studies.

2 Keywords

Inflow Boundary Conditions; Direct Numerical Simulation; Spray A; Droplet Analysis; Plain Orifice

3 Introduction

The role of boundary conditions (BC) in Direct Numerical Simulation (DNS) is widely accounted to be among the most important factors determining the simulation outcome. In DNS of multiphase flows, the inflow BC have been proven to affect the primary atomization [1] which, ultimately, affect the spray morphology as well as its turbulence field [2,3]. Furthermore, an assessment on the type of inflow BC can be made as many have been investigated along the years [4].

In many atomizers the nozzle flow is difficult to estimate due to the complexity of the device and the lack of experimental data for the incomplete development of the turbulent flow within the confined region. For example, automotive injector geometries are difficult to reliably validate against experiments and the turbulent field can not be, in most occasions, considered as a reliable BC.

For this reason Menard et al. [3] proposed the use of a synthetic turbulence inflow BCs, developed by Klein et al. [5], which has been further explored by the authors in [1]. On the other hand, this BC produces a turbulent structures that are homogeneous, hence neglecting the inherit anisotropic nature of the turbulent structures developed in a boundary layer [6]. The method provides also the chance to adapt the correlation tensor for matching anisotropic flow features, but this option is often overlooked due to lack in information. Other interesting methods are listed in literature, e.g.[1,4].

The most reliable inflow BC is, when possible, a whole simulation of the nozzle, but for the reasons previously discussed, is not always feasible. Still, it is a legitimate question whether or not a turbulent inflow condition, such the one proposed in [5], may be sufficiently representative of the real turbulent structures as well as accurately representing a corresponding atomization.

In this context, the present work investigates and compares the effects on the primary atomization of the inflow synthetic BC proposed by [5] (hereafter named SBC) in respect to the ones generated by a mapped inflow BC (hereafter named MBC) obtained from a Large Eddy Simulation (LES) of a periodical pipe flow. While the DNS simulation will be executed using the exact same parameters and solvers, presented in section 4.1, the LES simulation setup (as well as the mapping procedure) will be explained in section 4.2 . The comparison will be made merely by granulometric analysis, for which the analysis algorithm will be presented in section 5.

4 Methodologies

4.1 DNS Methodology

The code PARIS-Simulator [7] has been used to simulate the spray primary atomization in a quiescent environment. The code resolves the equations of an incompressible flow on a cartesian grid using the following state equations:

$$\nabla \cdot \boldsymbol{u} = 0 \tag{1}$$

$$\rho(\partial_t \boldsymbol{u} + \boldsymbol{u} \cdot \nabla \boldsymbol{u}) = -\nabla p + \nabla \cdot (2\mu \boldsymbol{D}) + \sigma \beta \delta_s \boldsymbol{n} \tag{2}$$

Where ρ is the fluid density, $\boldsymbol{u}$ is the velocity field, p is the pressure field, μ is the fluid dynamic viscosity and the deformation tensor is described by $\boldsymbol{D} = (\partial_i u_j + \partial_j u_i)/2$. The surface tension is accounted for in the last term on the right hand side term of Eq. (2), being σ the surface tension, β the liquid surface curvature, δ_s a Dirac distribution function that concentrate the effects of the source term on the liquid surface and, finally, $\boldsymbol{n}$ is the liquid surface normal vector.

The Volume of Fluid (VOF) method is used to model the multiphase nature of the flow. This method, as many in which a scalar tracker (or colour function) for the liquid is used, uses an advection equation for the volume fraction C:

$$\partial_t C + \boldsymbol{u} \cdot \nabla C = 0 \tag{3}$$

By using Eq. 3, the density and the viscosity can be computed as an arithmetic mean:

$$\rho = C\rho_l + (1 - C)\rho_g \tag{4}$$

$$\nu = C\nu_l + (1 - C)\nu_g \tag{5}$$

Where l and g subscripts represent respectively the liquid and the gas phase properties.

	Values
Spray mean velocity	$100\ m/s$
Injector diameter	$0.09\ mm$
Fuel viscosity	$1.34 \cdot 10^{-3}\ Pa \cdot s$
Fuel density	$750\ kg/m^3$
Fuel/ Nitrogen Surface Tension	$2.535 \cdot 10^{-5}\ N/m$
Nitrogen viscosity	$1.85 \cdot 10^{-5}\ Pa \cdot s$
Nitrogen density	$22.8\ kg/m^3$
Cell size	$2.343\ \mu m$
x *–Length*	$2.4\ mm$
y/z *–Length*	$1.2\ mm$

Table 1: Simulation parameters.

More information on the code may be found in [8,9] while the method for solving the VOF algorithm is presented in [10].

For both cases simulated, the simulation setup is identical while the only changing factor is the inlet BC. Table 1 shows the simulation parameter.

4.2 The Large Eddy Simulation of a pipe flow

The objective of the LES simulation is to develop a statistical stationary solution of a pipe flow (of the same diameter of the nozzle), while accurately simulate all the scales of motion that can be meaningful in a spray primary atomization simulation. In other words, any turbulent structure for which the minimum size is comparable with the DNS mesh size needs to be accurately solved, hence be above the sub grid. On the other hand, while the wall zero-velocity will be reproduced in the DNS simulation, the very first y+ values will not be represented in the spray simulation due to its mesh grid resolution. While extending the study of sub-Kolmogorov scale size particles would be extremely interesting [11], it is highly demanding and likely unfeasible nowadays. Therefore, the mesh size for the LES simulation was balanced in order to be able to obtain a reasonably accurate solution while maintaining the cost of the simulation and of its post-processing affordable. A snapshot of the velocity field could be found in Figure 1, where the filtered velocity $\tilde{u}$ is showed

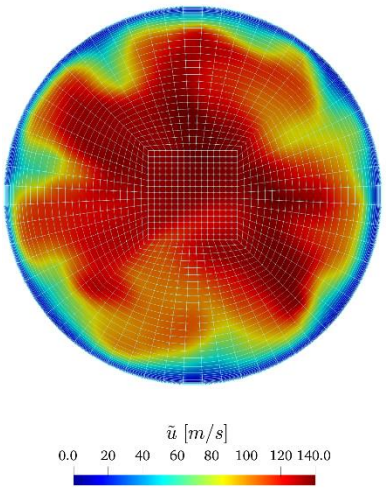

Figure 1: Velocity snapshot of a section in the pipe centre.

The simulation has been performed using OpenFOAM by using the same properties as for the DNS simulations (see Table 1). The solver *pisoFoam* was used and the simulation was performed for a total of 90 washouts (with a timestep of 20 ns). The LES sub-grid model used was the WALE (Wall-Adapting Local Eddy-viscosity). Once the simulation reached the statistically stationary state, the simulation turbulent statistics were checked in order to validate the results and have a similar mean velocity profile, as well as velocity deviation while using the two BCs. The comparison of the velocity root mean square (u_{rms}) and the mean velocity ($\langle U \rangle$), both made dimensionless by the y^+, are showed Figure 2

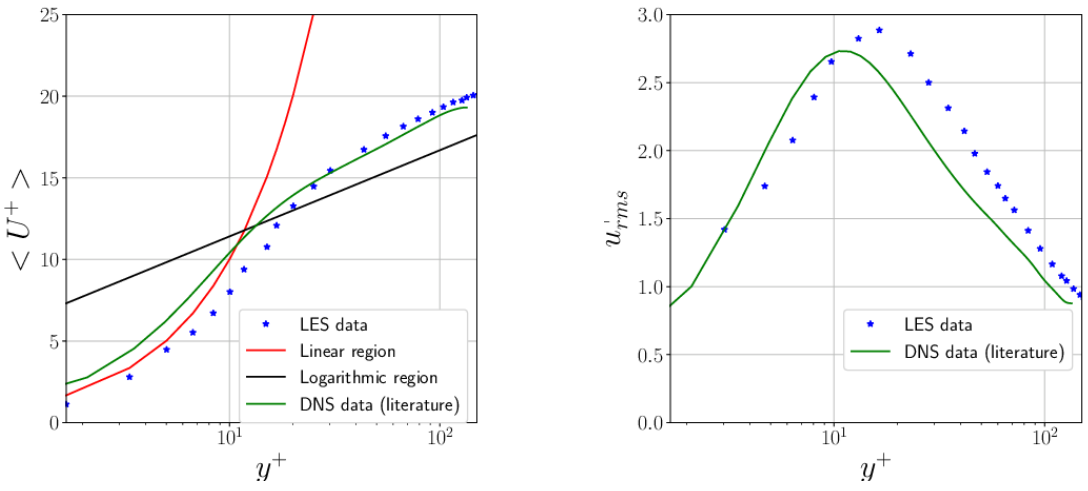

Figure 2: Validation of the turbulent statistics of the pipe LES simulation, namely the averaged dimensionless velocity field (left) and the velocity root mean squares (right).

Once the simulation is validated, the results are interpolated into a Cartesian mesh which is fed to ParisSimulator every 5 time steps. Finally, it is worth mentioning that the values of turbulent lengthscale L and turbulent intensity I for the SBC case have been directly calculated from the results of the LES simulation.

4.3 Granulometry determination methodology

Regardless of the inflow BC used, the simulation output is stored every $0.5\ \mu s$ during the transient (until the spray reaches the end of the axial domain) and then each $10\ \mu s$ in order to perform significant averages for a total simulation time of $0.3\ ms$.

In order to derive the granulometric analysis, the whole domain is analysed. In a first place, the spray liquid core that is still connected to the nozzle outlet is removed. Then, the whole domain is scanned recursively and every liquid structure is identified. In order to have an unambiguous definition of a “droplet” we consider it as a continuous liquid structure defined by free surfaces. This definition implies that any liquid structure that is not connected to the nozzle is considered a droplet (hereafter used terms for any granulometry analysis results).

This method has been chosen aiming at being useful from both an experimental and a numerical standpoint. From an experimental standpoint, a droplet can be considered as any liquid structure that will not appear in an optical connectivity analysis. From a numerical standpoint, this means that this result may be directly useful for improving the Discrete Droplet Model (DDM).

Finally, all the droplets are located in the corresponding center of mass of the liquid structure that represents and its velocities are averages of the velocity components on each cell that compose the droplet.

5 Results

5.1 General considerations over the atomization process

Figure 3 shows the results of the granulometry analysis in an instantaneous snapshot. The shadowed contour of the VOF is showed, as well as each equivalent droplet detected by the algorithm with its corresponding speed. As it can be seen in this figure, many large size droplets can be observed close to the spray axis. These are mostly large liquid structure derived from the axial core breakup that, despite the large size, should be considered as a result of primary atomization. These structures are still characterized by a high energy content and are likely to generate other droplets downstream due to secondary atomization.

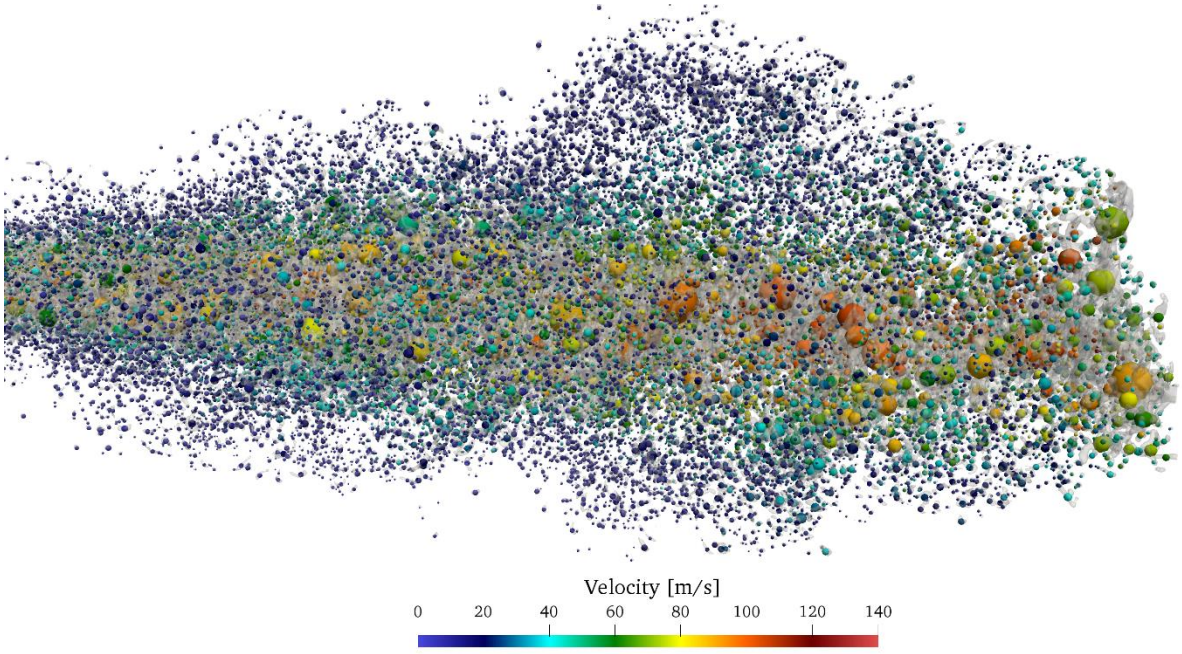

Figure 3: Snapshot of the granulometric analysis where all the liquid structures have been converted into equivalent droplets.

On the spray periphery, a significant number of droplets of small size and characterized by low velocity can be observed. While these droplets are the result of secondary breakup, they are also most of the droplets (as it will be demonstrated later on). The low energy content of these droplets (as can be observed in Figure 3, most of the small droplets are characterized by low velocity) decrease the possibility of further secondary breakup, while coalescence is still very possible, especially closer to the spray centerline. On the other hand, the analysis of a snapshot sequence reveals that most of the smallest droplets, that define the spray periphery, are generated by the tip breakup. At the tip, most of the liquid structures are actually represented by the sheets breaking up due to aerodynamic forces. The tear of this liquid sheets generates smaller droplet that are then pushed on the sides by the main vortex tip.

These considerations should lead to the conclusion that the spray outer region would behave as a particle laden flow with particles larger than the Kolmogorov scale η, with a main advection flow. The chance of evaluating the spray in such a way is not useful to understand the spray transient behaviour per se, but it may be interesting in order to assess how the droplets are affecting the turbulent field generated by the main flow and how it may prompt further atomization and/or coalescence, which is ultimately one of the main aspect to understand in combustion applications.

Furthermore, it is worth noticing that this analysis is not able to capture sub-Kolmogorov scale particles, which should be addressed in future studies.

5.2 Granulometric analysis

The analysis has been performed for $260\ \mu s$ after the spray have completely penetrate the simulation domain. The total number of droplet detected is quite higher for the MBC case (29000 ca.) than for the SBC case (26000 ca), denoting how, overall, the MBC is able to generate a higher shear stress (hence atomization), likely due to more turbulent energy injected overall at the various turbulent scales.

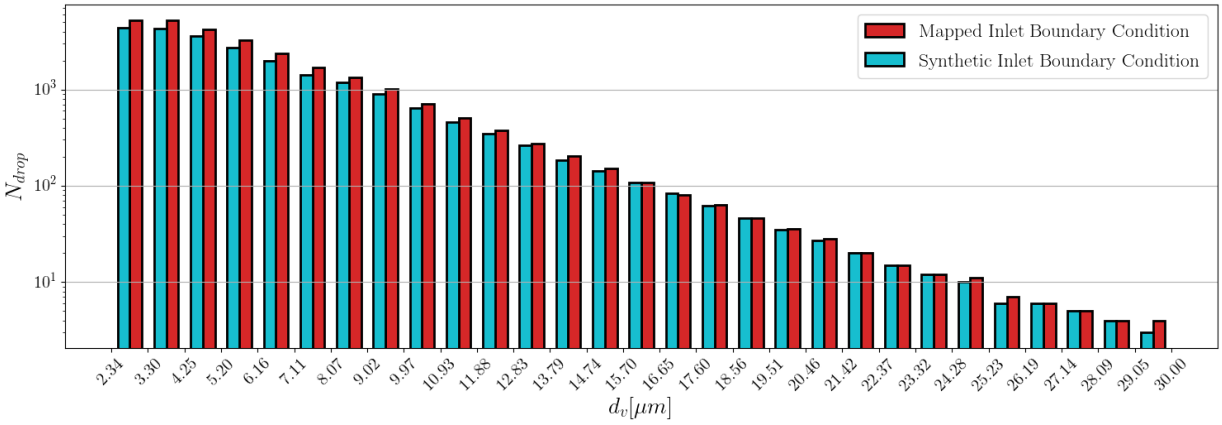

Figure 4: Droplet size (expressed using $\boldsymbol{d_v}$) distribution averaged in time.

Figure 4 shows the comparison of the droplet size distribution, where the droplet diameter is based on the volume (that can be calculated using the color function) and is calculated as:

$$d_v = \sqrt[3]{\frac{6V}{\pi}}. \tag{6}$$

It appears evidently that, despite a significant difference in the droplet generation (more than 10% in droplet generation for the MBC case) the general trend is definitely similar, especially in the larger droplet range, also it is worth mentioning that the droplet diameter are similar to values measured in Argonne National Lab [12]. This suggests that the larger turbulent structures, that accounts for most of the turbulent kinetic energy, are well captured by the SBC. In fact, these turbulent structures are the only ones that are likely to have enough energy to generate large structures breakup.

The fact that the smaller droplets are generated more abundantly in the MBC case would suggest two main considerations. In a first place, as the droplet with smaller diameter are likely the ones with lower kinetic energy (see Figure 3) this behaviour is likely the result of a faster atomization process occurring in the MBC case (and will be addressed in the following section). Secondly, as already discussed for larger structures, the presence of small droplets is likely generated by a combination of smaller and larger turbulent structures. While the latest have already been addressed and are likely to be accurately represented in the SBC case, smaller structure are likely to be the cause of the different atomization regime. In other words, the smallest turbulent structure in the MBC are likely at a different spatial or temporal frequency then the ones simulated in the SBC.

Figure 5 shows the temporal evolution of the number of droplets divided in series, each one characterized by a range of droplet diameters (reported in the legend). Until the spray reaches the whole domain penetration ($x = 2.4mm$) at approximately $t = 0.025\ ms$. all the series show a pretty neat linear behaviour. When the complete spray penetration is reached, the smaller the droplet size, the more its total count saturates to a stationary value. It could immediately be noted that smaller droplets are always largely predominant, and the droplet generation slope is always greater than in larger droplets.

For the same droplet size range, MBC is always neatly generating more droplets than SBC but the overall behaviour is always the same. This information coupled with the results highlighted in Figure 4 indicates a significant and non-trivial aspect of the two different BC. In fact, it shows that the ad-hoc calibration of the SBC parameters allows for capturing the macro dynamic of the spray atomization but the offset is likely given by the usage of the hypothesis of homogeneous turbulence for SBC, while MBC clearly shows elongated turbulent structures, hence promoting the possibilities of strong anisotropy at the larger scales.

The observation of this behaviour, together with Figure 3 and Figure 4, suggest the following scenario:

- Most of the smallest droplet are generated by the primary atomization regime induced by the spray tip penetration. Here a significant atomization is produced by a strong turbulent field which is advected by the

main flow. Most of the droplets are then slowed down by the opposite direction of the main flow and the spray tip vortex. After the spray stop penetrating, the generation of the smallest droplets stops and the total number stabilizes. In fact, a smaller number of droplets is still produced in the spray central region where the high turbulent field guarantee the generation and propagation of surface instabilities on the liquid structures, hence atomization.

- Average size droplets, on the other hand, keep been generated at a constant rate, hence it is likely that the main mechanism that triggers their formation is coalescence.
- The droplet of very large size (liquid structures) are periodically renewed by the injection of liquid in the domain. They continuously breakup and join with smaller droplets, but ultimately their number is almost costant. Due to the significant time required for the whole process to take place, most of the larger droplets are likely to exit the domain after been advected by the main flow.

It is interesting to notice that both the MBC and SBC cases present the same atomizing behaviour but the curves (represented with the same colour) are presenting the same behaviour while maintaining a separation between the stationary values that would justify the results presented in Figure 4.

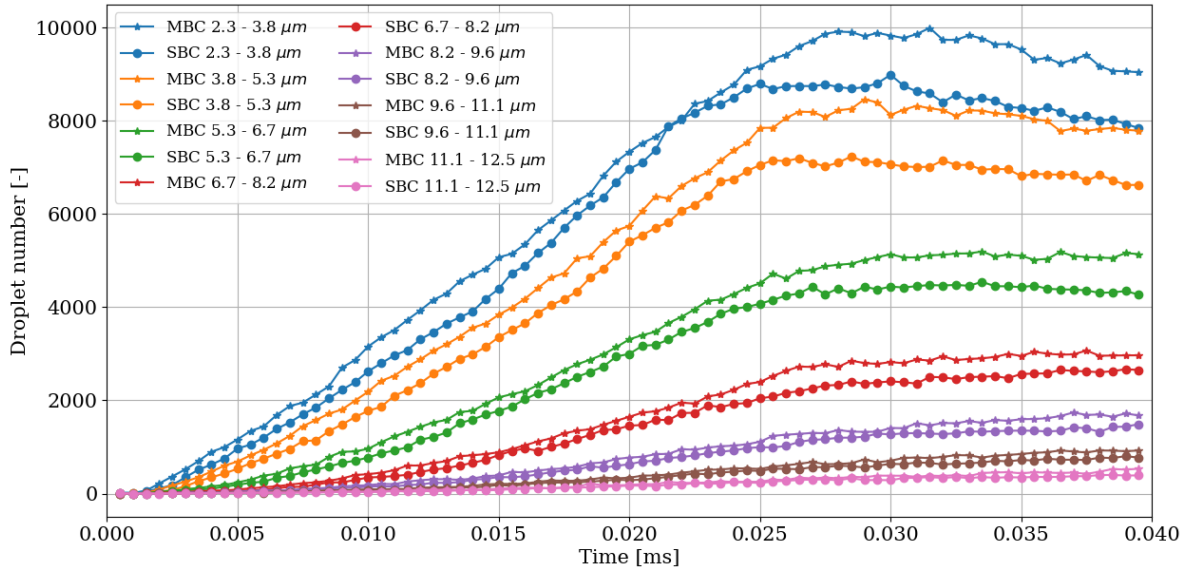

Figure 5: Temporal evolution of droplet generated during the spray penetration transient

From the result presented, both a temporal evolution of the droplet generated, as well as their distribution can be analysed. On the other hand, if we assume the droplet distribution to be perfectly linear, the biggest unknown would be the determination of the curve slope and how it relays to the droplet size range, the injection conditions (in terms, for example of dimensionless numbers) and how it would evolve for a complete spray penetration.

6 Conclusions and future outcomes

In this work, we compared two different inlet boundary conditions for the simulation of an atomizing spray. Although a significant variation in the total amount of atomized droplet is found, the overall dynamic is well preserved. For this reason, for many applications, this BC could be used successfully as far as the main objective of the work is capturing trends and behaviour in the atomization process. The complete analysis of this simulations, via their spectral behaviour, mass and velocity radial distributions and turbulent kinetic energy balance is still required to provide a complete and detailed explanation of both the differences observed as well as the similarity in trends.

In any case, such a post-process procedure opens the way to a statistical analysis of the atomization process, which will result in interesting and usable data both for comparison with experiments, as well as computational results. The main goal in future works will be centred on a statistical description of the atomization process for the stationary as well as the transient for the spray penetration. Furthermore, a join analysis of the interaction between turbulence and atomization and droplet propagation can be performed by using the data presented in this work.

7 Acknowledgments

This research has been partially funded by Spanish *Ministerio de Economía y Competitividad* through project TRA2015-67679-c2-1-R. Additionally, the authors thankfully acknowledge the computer resources at MareNostrum3 (Barcelona Supercomputing Center) and their technical support provided by FI-2017-2-0035 and TITAN (Oak Ridge Leadership Computing Facility) in the frame of the project TUR124.

8 References

[1] Salvador, F. J., Ruiz, S., Crialesi-Esposito, M., and Blanquer, I., 2018, “Analysis on the Effects of Turbulent Inflow Conditions on Spray Primary Atomization in the Near-Field by Direct Numerical Simulation,” Int. J. Multiph. Flow, **102**, pp. 49–63.

[2] Shinjo, J., and Umemura, A., 2010, “Simulation of Liquid Jet Primary Breakup: Dynamics of Ligament and Droplet Formation,” Int. J. Multiph. Flow, **36**(7), pp. 513–532.

[3] Ménard, T., Tanguy, S., and Berlemont, A., 2007, “Coupling Level Set/VOF/Ghost Fluid Methods: Validation and Application to 3D Simulation of the Primary Break-up of a Liquid Jet,” Int. J. Multiph. Flow, **33**(5), pp. 510–524.

[4] Sagaut, P., 2006, *Large Eddy Simulation for Incompressible Flows: An Introduction*, Springer Science & Business Media.

[5] Klein, M., Sadiki, A., and Janicka, J., 2003, “A Digital Filter Based Generation of Inflow Data for Spatially Developing Direct Numerical or Large Eddy Simulations,” J. Comput. Phys., **186**(2), pp. 652–665.

[6] Saddoughi, S. G., and Veeravalli, and S. V., 1994, “Local Isotropy in Turbulent Boundary Layers at High Reynolds Number,” J. Fluid Mech., **268**, pp. 333–372.

[7] Arrufat, T., Bondino, I., and Zaleski, S., 2014, “SPE-172025-MS Developments on Relative Permeability Computation in 3D Rock Images,” Dev. Relat. Permeability Comutation 3D Rock Images.

[8] Ling, Y., Fuster, D., Zaleski, S., Tryggvason, G., and Zaleski, S., 2019, “A Two-Phase Mixing Layer between Parallel Gas and Liquid Streams: Multiphase Turbulence Statistics and Influence of Interfacial Instability,” J. Fluid Mech., **859**, pp. 268–307.

[9] Tryggvason, G., Scardovelli, R., and Zaleski, S., 2011, *Direct Numerical Simulations of Gas--Liquid Multiphase Flows*, Cambridge University Press.

[10] Scardovelli, R., and Zaleski, S., 1999, “Direct Numerical Simulation of Free-Surface and Interfacial Flow,” Annu. Rev. Fluid Mech., **31**(1), pp. 567–603.

[11] Elghobashi, S., 2018, “Direct Numerical Simulation of Turbulent Flows Laden with Droplets or Bubbles,” Annu. Rev. Fluid Mech., **51**(1), pp. 217–244.

[12] Kastengren, A., Ilavsky, J., Viera, J. P., Payri, R., Duke, D. J., Swantek, A., Tilocco, F. Z., Sovis, N., and Powell, C. F., 2017, “Measurements of Droplet Size in Shear-Driven Atomization Using Ultra-Small Angle x-Ray Scattering,” Int. J. Multiph. Flow, **92**.